ELSEVIER

Robotics and Autonomous Systems 34 (2001) 179–202

Robotics and Autonomous Systems

www.elsevier.com/locate/robot

Classification of the Dubins set☆

Andrei M. Shkel [a,*], Vladimir Lumelsky [b]

[a] *Department of Mechanical and Aerospace Engineering, University of California, 4208 Engineering Gateway Building, Irvine, CA 92717-3975, USA*

[b] *Department of Mechanical Engineering, University of Wisconsin-Madison, Madison, WI 53706, USA*

Received 14 August 1998; received in revised form 13 November 2000

Communicated by T.C. Henderson

Abstract

Given two points in a plane, each with a prescribed direction of motion in it, the question being asked is to find the shortest smooth path of bounded curvature that joins them. The classical 1957 result by Dubins gives a sufficient set of paths (each consisting of circular arcs and straight line segments) which always contains the shortest path. The latter is then found by explicitly computing all paths on the list and then comparing them. This may become a problem in applications where computation time is critical, such as in real-time robot motion planning. Instead, the logical classification scheme considered in this work allows one to extract the shortest path from the Dubins set directly, without explicitly calculating the candidate paths. The approach is demonstrated on one of two possible cases that appear here — when the distance between the two points is relatively large (the case with short distances can be treated similarly). Besides computational savings, this result sheds light on the nature of factors affecting the length of paths in the Dubins problem, and is useful for further extensions, e.g. for finding the shortest path between a point and a manifold in the corresponding configuration space. © 2001 Published by Elsevier Science B.V.

Keywords: Computational geometry; Geometric algorithms; Shortest path problems; Robotics; Nonholonomic motion

1. Introduction

Consider the problem of finding the shortest smooth path between two points in the plane, the *initial and final points*, P_i and P_f. Each point is associated with its own *orientation angle*, α and β, respectively, which defines the prescribed direction of motion in it (see Fig. 1). The combinations (P_i, α) and (P_f, β), called the *initial and final configurations*, define two points in the corresponding *configuration space* (*C-space*), and present the problem's boundary conditions. Given (P_i, α) and (P_f, β), the task is to find the shortest smooth path from P_i to P_f, such that it starts and ends with the directions of motion α and β, respectively, and the path curvature is limited by $1/\rho$, where ρ is the minimal radius of turning.

This kind of tasks appear in various applications, such as when joining pieces of railways [1] or planning two- and three-dimensional pipe networks. In robotics, this problem plays a central role in most of the work on nonholonomic motion planning [2–4].

☆ This work was supported by the National Science Foundation Grant IRI-9220782 and the Sea Grant Program (National Oceanic and Atmospheric Administration, US Department of Commerce, Grant NA46RG048).

* Corresponding author.

E-mail addresses: ashkel@uci.edu (A.M. Shkel), lumelsky@robios.me.wisc.edu (V. Lumelsky).

0921-8890/01/$ – see front matter © 2001 Published by Elsevier Science B.V.

PII: S0921-8890(00)00127-5

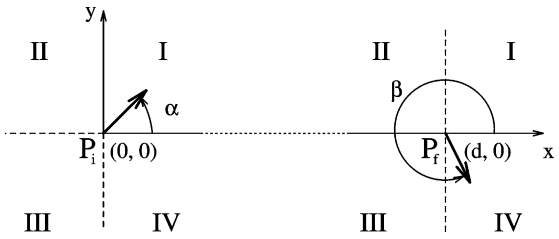

Fig. 1. The coordinate system, the initial configuration (P_i, α) and the final configuration (P_f, β). Possible orientation angles are divided into four quadrants.

The complete solution to this problem was first reported in an elegant paper by Dubins [5] in 1957. He showed that any geodesic (i.e. the shortest path) consists of exactly three path segments and presents a sequence *CCC* or *CSC*, where *C* (for "circle") is an arc of radius ρ, and *S* (for "straight") is a line segment. Each arc *C* has two options — turning left or turning right. Denote those *L* and *R*, respectively, and the line segment by *S*. The Dubins set, $\mathcal{D}$, includes six *admissible paths* (or words), $\mathcal{D} = \{LSL, RSR, RSL, LSR, RLR, LRL\}$. Furthermore, Dubins' theorem states that in order to be a candidate for the optimal path, each arc must be of the minimal allowed radius ρ.

Using advanced calculus, this result of Dubins was later proved by Reeds and Shepp [6]. Also, Boissonnat et al. [7] proved this result from the standpoint of optimal control, by making use of the powerful Pontryagin's optimality principle [8]. The more difficult case in which the path from (P_i, α) to (P_f, β) can be further shortened by allowing reversals of motion (and thus introducing cusps) was first considered in the same work by Reeds and Shepp [6]. They showed that the initial and final configurations define a sufficient set of 48 paths which contains the optimal path. The technique presented in [9] allows one to pick the optimal solution out of this set of 48 by partitioning the *C*-space into multiple domains such that a single path type is associated with 150 elements and two path types are associated with the other 11 elements.

An alternative approach to the problem with reversals was proposed by Soueres and Laumond [10]. They tie the Pontryagin's optimality principle with geometric reasoning, and arrive at the optimal solution via partitioning of *C*-space into regions with uniform properties of path optimality.

In the context of robotics, the original Dubins problem of constructing a smooth path has a significance of its own. In many motion planning tasks, such as in the aircraft control, motion reversals are not feasible. Or, if the shortest time path, rather than the shortest path, is desired, the solution is likely to be a smooth path, because the deceleration, stop, and acceleration at the reversal cusps add time to the path execution. Unfortunately, Dubins' problem with smooth paths is not a subset of the Reeds–Shepp's problem — the sufficient set of the former is not contained in the sufficient set of the latter. Also, the techniques proposed in [9,10] are not directly applicable to the smooth path case.

To use Dubins's result for the shortest path calculation, one would need to explicitly calculate the lengths of all arcs and straight line segments in the Dubins set, and then choose the shortest of the computed paths. The time necessary for this calculation may become a bottleneck in time-constrained applications, as e.g. in real-time robot motion planning — which is one motivation for this work. Another motivation comes from problems where one looks for the shortest path from a point to a manifold in the *C*-space. For example, in sensor-based obstacle avoidance, when planning an arrival to some intermediate point *P* on the obstacle boundary, the current sensing data may suggest that in order not to collide with the obstacle, the orientation angle β at *P* must be within some sector of angles (which may include, e.g. the tangent to the obstacle at *P*). Finding the shortest path to *P* under this constraint corresponds to finding the shortest path to a line in *C*-space.

In this work, we propose a scheme which allows one to select the shortest path from the Dubins set $\mathcal{D}$ directly, without the usual exhaustive calculation of its elements. The scheme is based on a rather suggestive fact, developed in Section 5, that the elements of the Dubins set can be classified into a small number of the so-called *equivalency groups*, based on the angle quadrants of the corresponding pairs of the initial and final orientation angles. Each equivalency group consists of a few *classes* of paths, such that any path in a group is equivalent, up to an orthogonal

transformation, to any other path in the same group. This means that the optimal path analysis can be reduced to fewer terms. Further, a simple logical classification of the equivalency groups can be built which points directly to the optimal path.

Below, d is the Euclidean distance between the initial and final points P_i and P_f. A rectangular coordinate system (x, y) is chosen such that its origin is $P_i = (0, 0)$ and the positive direction of x-axis is toward $P_f = (d, 0)$ (Fig. 1). The initial and final orientation angles, α and β, are measured counter-clockwise, with respect to the positive direction of x-axis. Without loss of generality, assume a unit radius of the minimum turning circle, $\rho = 1$ (any other ρ can be reduced to 1 by the scaling $d = D/\rho$, where D is the actual distance between P_i and P_f). The initial and final arc segments (of radius ρ) in the Dubins set are denoted C_{il}, C_{ir}, C_{fl}, C_{fr} (where i and f stand for "initial" and "final", and r and l — for "right" and "left").

The analysis necessary for solving our classification problem turns out to become simpler if it is divided into two cases, which can be called the *long path case* and the *short path case*. Our approach is equally applicable to both cases, with minor differences between the resulting computational schemes. For the sake of example, we consider here only one case, the *long path case*, which seems to be of more interest from the standpoint of applications and the computational savings. More precisely, the "long paths" are those where the distance d between the points P_i and P_f satisfies the condition of non-intersection of the four circles above, $\{C_{il} \cup C_{ir}\} \cap \{C_{fl} \cup C_{fr}\} = \emptyset$. This covers all cases when $d \geqslant 4\rho$ and some cases when $d < 4\rho$ (see Fig. 4 and Proposition 5).

We first develop, in Section 2, a proper specification scheme for admissible paths. The notion of an equivalency group is then introduced in Section 3, and the scheme for classifying the Dubins set is fully developed in Section 4. This work's main result which makes this classification possible and becomes the logical scheme for finding the shortest path is summarized in Section 4.

2. Admissible paths and their specification

Given a path from the initial to the final configuration, the position of a point on the path is fully specified by its Cartesian location $x(\tau)$, $y(\tau)$, where the parameterization variable τ can be interpreted as time or the length of path traversed from P_i with unit velocity. Assume

$\tau_i = 0$, i.e. $P_i = P(\tau_i) = P(0)$;
the point on the path can move only "forward", from P_i toward P_f;
it moves with the unit speed;
the orientation angle (direction of motion) cannot change faster than $1/\rho$ radian per time unit,
where $\rho = 1$ is the minimal turning radius.

Following [5], an *admissible path* is defined as a continuously differentiable curve which is either (i) an arc of a circle of radius 1, followed by a line segment, followed by an arc of a circle of radius 1, or (ii) a sequence of three arcs of circles of radius 1, or (iii) a subpath of a path of type (i) or (ii). A list of admissible paths forms a sufficient set of optimal paths.

To specify admissible paths, we introduce three elementary motions: turning to the left, turning to the right (both along a circle C of radius 1), and straight line motion S. Also needed will be three corresponding operators, L_v (for left turn), R_v (for right turn), S_v (for straight), which transform an arbitrary point $(x, y, \phi) \in \mathbb{R}^3$ into its corresponding image point in $\mathbb{R}^3$,

$$\begin{aligned} L_v(x, y, \phi) &= (x + \sin(\phi + v) - \sin\phi,\ y - \cos(\phi + v) + \cos\phi,\ \phi + v), \\ R_v(x, y, \phi) &= (x - \sin(\phi - v) + \sin\phi,\ y + \cos(\phi - v) - \cos\phi,\ \phi - v), \\ S_v(x, y, \phi) &= (x + v\cos\phi,\ y + v\sin\phi,\ \phi), \end{aligned} \tag{1}$$

where index v indicates that the motion has been along the (C or S) segment of length v. With these elementary transformations, any path in the Dubins set $\mathcal{D} = \{LSL, RSR, RSL, LSR, RLR, LRL\}$ can be expressed in terms of

the corresponding equations. In the coordinate system chosen, the initial configuration of each path is at $(0, 0, \alpha)$ and the final configuration at $(d, 0, \beta)$. For example, a path made of segments L, R and L, of the lengths t, p, q, respectively, which starts at point $(0, 0, \alpha)$, must end at $L_q(R_p(L_t(0, 0, \alpha))) = (d, 0, \beta)$. The length $\mathcal{L}$ of the path can be defined as the sum of lengths t, p and q of its constituent segments,

$$\mathcal{L} = t + p + q. \tag{2}$$

Our goal is to classify the elements of set $\mathcal{D}$ based on the boundary conditions, with the purpose of replacing the explicit computation of all candidates for the shortest path with a simple logical procedure that would directly produce the shortest path. To this end, we will now consider elements of $\mathcal{D}$ one-by-one and derive the operator equations for the length of each path.

1. $L_q(S_p(L_t(0, 0, \alpha))) = (d, 0, \beta)$. By applying the corresponding operators (1), this first path in $\mathcal{D}$ can be represented by a system of three scalar equations:

$$\begin{aligned} &p\cos(\alpha + t) - \sin\alpha + \sin\beta = d,\\ &p\sin(\alpha + t) + \cos\alpha - \cos\beta = 0,\\ &\alpha + t + q = \beta \{\mathrm{mod}\, 2\pi\}. \end{aligned}$$

The solution of this system with respect to the segments t, p and q is found as

$$\begin{aligned} t_{lsl} &= -\alpha + \arctan\frac{\cos\beta - \cos\alpha}{d + \sin\alpha - \sin\beta} \{\mathrm{mod}\, 2\pi\},\\ p_{lsl} &= \sqrt{2 + d^2 - 2\cos(\alpha - \beta) + 2d(\sin\alpha - \sin\beta)},\\ q_{lsl} &= \beta - \arctan\frac{\cos\beta - \cos\alpha}{d + \sin\alpha - \sin\beta} \{\mathrm{mod}\, 2\pi\}. \end{aligned} \tag{3}$$

Using definition (2), the length of the path *LSL* as a function of the boundary conditions can be now written as

$$\mathcal{L}_{lsl} = t_{lsl} + p_{lsl} + q_{lsl} = -\alpha + \beta + p_{lsl}. \tag{4}$$

2. $R_q(S_p(R_t(0, 0, \alpha))) = (d, 0, \beta)$. Using (1), we obtain the corresponding scalar equations:

$$\begin{aligned} &p\cos(\alpha - t) + \sin\alpha - \sin\beta = d,\\ &p\sin(\alpha - t) - \cos\alpha + \cos\beta = 0,\\ &\alpha - t - q = \beta \{\mathrm{mod}\, 2\pi\}. \end{aligned}$$

The solution of this system, i.e. the lengths of the corresponding segments, is

$$\begin{aligned} t_{rsr} &= \alpha - \arctan\frac{\cos\alpha - \cos\beta}{d - \sin\alpha + \sin\beta} \{\mathrm{mod}\, 2\pi\},\\ p_{rsr} &= \sqrt{2 + d^2 - 2\cos(\alpha - \beta) + 2d(\sin\beta - \sin\alpha)},\\ q_{rsr} &= -\beta(\mathrm{mod}\, 2\pi) + \arctan\frac{\cos\alpha - \cos\beta}{d - \sin\alpha + \sin\beta} \{\mathrm{mod}\, 2\pi\}, \end{aligned} \tag{5}$$

and the path length is given by

$$\mathcal{L}_{rsr} = t_{rsr} + p_{rsr} + q_{rsr} = \alpha - \beta + p_{rsr}. \tag{6}$$

3. $R_q(S_p(L_t(0,0,\alpha))) = (d,0,\beta)$. Using (1), we obtain the corresponding scalar equations:

$$p\cos(\alpha+t) + 2\sin(\alpha+t) - \sin\alpha - \sin\beta = d,$$
$$p\sin(\alpha+t) - 2\cos(\alpha+t) + \cos\alpha + \cos\beta = 0,$$
$$\alpha + t - q = \beta \{\mathrm{mod}\, 2\pi\}.$$

The solution of this system is

$$t_{lsr} = \left(-\alpha + \arctan\left(\frac{-\cos\alpha - \cos\beta}{d + \sin\alpha + \sin\beta}\right) - \arctan\left(\frac{-2}{p_{lsr}}\right)\right) \{\mathrm{mod}\, 2\pi\},$$
$$p_{lsr} = \sqrt{-2 + d^2 + 2\cos(\alpha-\beta) + 2d(\sin\alpha + \sin\beta)}, \tag{7}$$
$$q_{lsr} = -\beta(\mathrm{mod}\, 2\pi) + \arctan\left(\frac{-\cos\alpha - \cos\beta}{d + \sin\alpha + \sin\beta}\right) - \arctan\left(\frac{-2}{p_{lsr}}\right) \{\mathrm{mod}\, 2\pi\},$$

and the path length is given by

$$\mathcal{L}_{lsr} = t_{lsr} + p_{lsr} + q_{lsr} = \alpha - \beta + 2t_{lsr} + p_{lsr}. \tag{8}$$

4. $L_q(S_p(R_t(0,0,\alpha))) = (d,0,\beta)$. Using (1), we obtain the corresponding scalar equations:

$$p\cos(\alpha - t) - 2\sin(\alpha - t) + \sin\alpha + \sin\beta = d,$$
$$p\sin(\alpha - t) + 2\cos(\alpha - t) - \cos\alpha - \cos\beta = 0,$$
$$\alpha - t + q = \beta \{\mathrm{mod}\, 2\pi\}.$$

The corresponding solution is

$$t_{rsl} = \alpha - \arctan\left(\frac{\cos\alpha + \cos\beta}{d - \sin\alpha - \sin\beta}\right) + \arctan\left(\frac{2}{p_{rsl}}\right) \{\mathrm{mod}\, 2\pi\},$$
$$p_{rsl} = \sqrt{d^2 - 2 + 2\cos(\alpha-\beta) - 2d(\sin\alpha + \sin\beta)}, \tag{9}$$
$$q_{rsl} = \beta(\mathrm{mod}\, 2\pi) - \arctan\left(\frac{\cos\alpha + \cos\beta}{d - \sin\alpha - \sin\beta}\right) + \arctan\left(\frac{2}{p_{rsl}}\right) \{\mathrm{mod}\, 2\pi\},$$

and the path length is given by

$$\mathcal{L}_{rsl} = t_{rsl} + p_{rsl} + q_{rsl} = -\alpha + \beta + 2t_{rsl} + p_{rsl}. \tag{10}$$

5. $R_q(L_p(R_t(0,0,\alpha))) = (d,0,\beta)$. Using (1), we obtain the corresponding scalar equations:

$$2\sin(\alpha - t + p) - 2\sin(\alpha - t) = d - \sin\alpha + \sin\beta,$$
$$-2\cos(\alpha - t + p) + 2\cos(\alpha - t) = \cos\alpha - \cos\beta,$$
$$\alpha - t + p - q = \beta \{\mathrm{mod}\, 2\pi\}.$$

The solution of this system is

$$\begin{aligned} t_{rlr} &= \alpha - \arctan\left(\frac{\cos\alpha - \cos\beta}{d - \sin\alpha + \sin\beta}\right) + \frac{p_{rlr}}{2} \{\mathrm{mod}\, 2\pi\}, \\ p_{rlr} &= \arccos \tfrac{1}{8}(6 - d^2 + 2\cos(\alpha - \beta) + 2d(\sin\alpha - \sin\beta)), \\ q_{rlr} &= \alpha - \beta - t_{rlr} + p_{rlr} \{\mathrm{mod}\, 2\pi\}, \end{aligned} \tag{11}$$

and the path length is obtained by substituting (11) into (2),

$$\mathcal{L}_{rlr} = t_{rlr} + p_{rlr} + q_{rlr} = \alpha - \beta + 2p_{rlr}. \tag{12}$$

6. $L_q(R_p(L_t(0, 0, \alpha))) = (d, 0, \beta)$. Using (1), we obtain the corresponding scalar equations:

$$\begin{aligned} &-2\sin(\alpha + t - p) + 2\sin(\alpha + t) = d + \sin\alpha - \sin\beta, \\ &2\cos(\alpha + t - p) - 2\cos(\alpha + t) = -\cos\alpha + \cos\beta, \\ &\alpha + t - p + q = \beta \{\mathrm{mod}\, 2\pi\}. \end{aligned}$$

The corresponding solution is

$$\begin{aligned} t_{lrl} &= \left(-\alpha + \arctan\left(\frac{-\cos\alpha + \cos\alpha}{d + \sin\alpha - \sin\beta}\right) + \frac{p_{lrl}}{2}\right) \{\mathrm{mod}\, 2\pi\}, \\ p_{lrl} &= \arccos \tfrac{1}{8}(6 - d^2 + 2\cos(\alpha - \beta) + 2d(\sin\alpha - \sin\beta)) \{\mathrm{mod}\, 2\pi\}, \\ q_{lrl} &= \beta (\mathrm{mod}\, 2\pi) - \alpha + 2p_{lrl} \{\mathrm{mod}\, 2\pi\}, \end{aligned} \tag{13}$$

and the path length is given by

$$\mathcal{L}_{lrl} = t_{lrl} + p_{lrl} + q_{lrl} = -\alpha + \beta + 2p_{lrl}. \tag{14}$$

3. Equivalency groups

We are now prepared to turn to the classification of the Dubins set $\mathcal{D}$. Divide the range of possible orientation angles (α, β) into four quadrants; Fig. 1: quadrant 1 corresponds to the range $[0, \pi/2]$, quadrant 2 to $[\pi/2, \pi]$, quadrant 3 to $[\pi, 3\pi/2]$, and quadrant 4 to the range $[3\pi/2, 2\pi]$. Since each of α or β can be in any of the four quadrants, together this produces 16 different combinations of possible quadrants. We represent those 16 by a 4×4 matrix, $\{a_{ij}\}$, where index i corresponds to the quadrant number of the initial, and index j that of the final orientation. Element a_{ij} therefore describes the *class* of all paths whose initial and final orientation angles (α, β) belong to the quadrants i and j, respectively. For example, the case $\alpha \in [0, \pi/2]$, $\beta \in [\pi/2, \pi]$ corresponds to the element a_{12} and covers all those paths whose orientation angles belong to the first and second quadrants, respectively.

It will be shown below that these 16 classes can be reduced to six independent clusters, called *equivalency groups*, such that an orthogonal transformation of any path in a given group changes it into a path in the same or a different class of the same group.

Dubins' main theorem [5] says that each (non-degenerate) candidate for the optimal path in set $\mathcal{D}$ must start with a piece of circle and end with a piece of circle (of radius $\rho = 1$, see above). Depending on the path in $\mathcal{D}$, the initial and the final circle can turn either left or right; we denote those C_{il}, C_{ir} and C_{fl}, C_{fr}, respectively. To proceed, we will need the following definition.

Definition. Two paths are topologically equivalent (denoted by "$\simeq$") if there exists an orthogonal transformation that maps one path into the other, with both paths sharing their respective initial and final points.

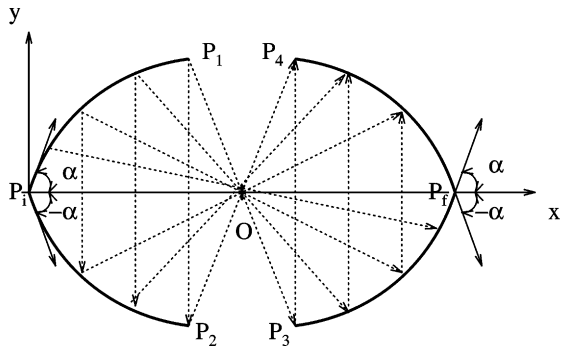

Fig. 2. Arcs P_iP_2 and P_3P_f are obtained by orthogonal transformations of the arc P_iP_1: the first is a mirror reflection of P_iP_1 with respect to line (P_iP_f), the second — the central symmetry reflection of P_iP_1 with respect to point O. Arc P_4P_f is obtained by applying a composition of both transformations.

Note that two equivalent paths are of the same length and allow equivalent parameterization. The following proposition relates the topological equivalency of paths and their initial/final configurations.

Proposition 1. *For any path connecting two points, $P(t_i, \alpha)$, $P(t_f, \beta)$, where (α, β) are the initial and final orientation angles, there exist another three paths which are topologically equivalent to it. Their corresponding orientation angles are $(-\alpha, -\beta)$, (β, α), and $(-\beta, -\alpha)$.*

To see this, consider a path that starts at an initial configuration (P_i, α) and is of the form $P_iP_1\cdots[-\alpha, -\beta]$; here the ellipsis "$\cdots$" reflect our emphasis on the segment P_iP_1 (Fig. 2). By applying a mirror reflection $\mathcal{G}_{(P_iP_f)}$ with respect to the line (P_iP_f), this path is transformed into the path $P_iP_2\cdots[-\alpha, -\beta]$. Similarly, by applying the central symmetry reflection $\mathcal{G}_{(O)}$ with respect to the midpoint O of segment $[P_i, P_f]$, the same path is transformed into $\cdots P_3P_f[\beta, \alpha]$. The composition of both transformations leads to

$$\mathcal{G}_{(O)}(\mathcal{G}_{(P_iP_f)}(P_iP_1\cdots[\alpha, \beta])) = \mathcal{G}_{(P_iP_f)}(\mathcal{G}_{(O)}(P_iP_1\cdots[\alpha, \beta])) = \cdots P_4P_f[-\beta, -\alpha]. \tag{15}$$

This general fact will be used below in the analysis of paths defined by set $\mathcal{D}$. Recall that those paths take a form either *CCC* or *CSC*, where *C* is an arc of a circle of radius ρ with options *L* and *R* (left and right), and *S* is a straight line segment. To distinguish between the first and the second arc segments in the path *CSC*, subscripts will be used, C_1SC_2.

Define the *conjugate* of C_1, denoted $\bar{C}_1$, as the complement of C, i.e. if $C_1 = R$ then its conjugate is $\bar{C}_1 = L$, and vice versa. The application of the orthogonal transformations $\mathcal{G}_{(P_iP_f)}$ and $\mathcal{G}_{(O)}$ leads to

$$\mathcal{G}_{(P_iP_f)}(C_1SC_2[\alpha, \beta]) = \bar{C}_1\bar{S}\bar{C}_2[-\alpha, -\beta], \qquad \mathcal{G}_O(C_1SC_2[\alpha, \beta]) = \bar{C}_2\bar{S}\bar{C}_1[\beta, \alpha].$$

Notice that the mirror reflection $\mathcal{G}_{(P_iP_f)}$ reverses the signs of angles α, β and changes the arc segments to their conjugates. The central symmetry reflection $\mathcal{G}_{(O)}$ has a triple effect: it switches orientations α and β, switches segments C_1 and C_2, and switches each segment to its conjugate. This relation can be proven rigorously by formalizing the operators $\mathcal{G}_{(P_iP_f)}$ and $\mathcal{G}_{(O)}$ and then applying them to the path presented in the general operator form, as e.g. $L_q(S_p(L_t(0, 0, \alpha))) = (d, 0, \beta)$.

Independent of the order of transformations, the composition of $\mathcal{G}_{(P_iP_f)}$ and $\mathcal{G}_{(O)}$ leads to

$$\mathcal{G}_{(O)}(\mathcal{G}_{(P_iP_f)}(C_1SC_2[\alpha, \beta])) = \mathcal{G}_{(P_iP_f)}(\mathcal{G}_{(O)}(C_1SC_2[\alpha, \beta])) = C_2SC_1[-\beta, -\alpha].$$

Using the above definition of topological equivalence, the following proposition defines the set of topologically equivalent paths.

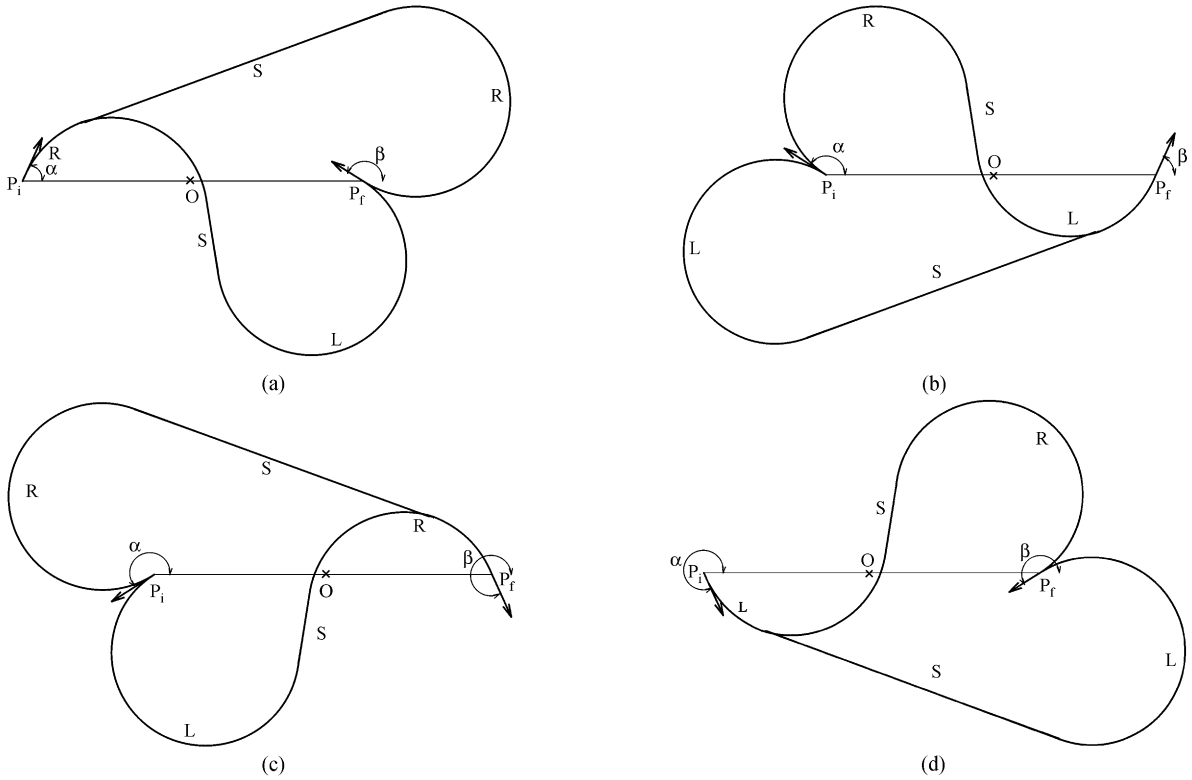

Fig. 3. An illustration for Proposition 2.

Proposition 2. *Given the path $C_1SC_1[\alpha, \beta]$, the composition of orthogonal transformations $\mathcal{G}_{(P_i P_f)}$ and $\mathcal{G}_{(O)}$ leads to the topologically equivalent paths*

$$C_1SC_2[\alpha, \beta] \simeq \bar{C}_1\bar{S}\bar{C}_2[-\alpha, -\beta] \simeq \bar{C}_2\bar{S}\bar{C}_1[\beta, \alpha] \simeq C_2SC_1[-\beta, -\alpha],$$

where α, β are the initial and final orientations, $\mathcal{G}_{(P_i P_f)}$ the mirror reflection with respect to line $(P_i P_f)$, $\mathcal{G}_{(O)}$ the central symmetry reflection with respect to the midpoint O of segment $[P_i, P_f]$, and "$\simeq$" the sign of equivalency.

Example. Consider the paths shown in Fig. 3. Initially there are two paths, $RSR[\alpha, \beta]$ and $RSL[\alpha, \beta]$ (Fig. 3(a)), where $\alpha \in [0, \pi/2]$, $\beta \in [\pi/2, \pi]$.

1. Consider first the path $RSR[\alpha, \beta]$. With the notation of Proposition 2, we have $C_1 = R$ and $C_2 = R$. The proposition gives the following set of topologically equivalent paths (see Fig. 3(a)–(d)):

$$\begin{aligned} RSR[\alpha \in [0, \pi/2], \beta \in [\pi/2, \pi]] &\simeq LSL[\alpha \in [3\pi/2, 2\pi], \beta \in [\pi, 3\pi/2]] \\ &\simeq LSL[\alpha \in [\pi/2, \pi], \beta \in [0, \pi/2]] \\ &\simeq RSR[\alpha \in [\pi, 3\pi/2], \beta \in [3\pi/2, 2\pi]]. \end{aligned}$$

2. Consider now an example $C_1 = R$, $C_2 = L$. By applying Proposition 2 to the path $RSL[\alpha, \beta]$ with $\alpha \in [0, \pi/2]$, $\beta \in [\pi/2, \pi]$ (Fig. 3(a)), we obtain three other paths (Fig. 3(b)–(d)):

$$RSL[\alpha \in [0, \pi/2], \beta \in [\pi/2, \pi]] \simeq LSR[\alpha \in [3\pi/2, 2\pi], \beta \in [\pi, 3\pi/2]]$$
$$\simeq RSL[\alpha \in [\pi/2, \pi], \beta \in [0, \pi/2]]$$
$$\simeq LSR[\alpha \in [\pi, 3\pi/2], \beta \in [3\pi/2, 2\pi]].$$

Proposition 3. *Given the path* $C_1SC_1[\alpha, \beta]$*, the individual orthogonal transformations* $\mathcal{G}_{(P_i P_f)}$, $\mathcal{G}_{(O)}$ *and their composition lead to the topologically equivalent paths* $C_1SC_2[\alpha, \beta]$, $\bar{C}_1\bar{S}\bar{C}_2[-\alpha, -\beta]$, $\bar{C}_2\bar{S}\bar{C}_1[\beta, \alpha]$, *and* $C_2SC_1[-\beta, -\alpha]$*, for which the following holds*:

$$\mathcal{L}_{c_1sc_2} = t_{c_1sc_2} + p_{c_1sc_2} + q_{c_1sc_2}, \qquad \mathcal{L}_{\bar{c}_1\bar{s}\bar{c}_2} = t_{\bar{c}_1\bar{s}\bar{c}_2} + p_{\bar{c}_1\bar{s}\bar{c}_2} + q_{\bar{c}_1\bar{s}\bar{c}_2},$$
$$\mathcal{L}_{\bar{c}_2\bar{s}\bar{c}_1} = t_{\bar{c}_2\bar{s}\bar{c}_1} + p_{\bar{c}_2\bar{s}\bar{c}_1} + q_{\bar{c}_2\bar{s}\bar{c}_1}, \qquad \mathcal{L}_{c_2sc_1} = t_{c_2sc_1} + p_{c_2sc_1} + q_{c_2sc_1},$$

and

$$t_{c_1sc_2} = t_{\bar{c}_1\bar{s}\bar{c}_2} = q_{\bar{c}_2\bar{s}\bar{c}_1} = q_{c_2sc_1}, \qquad p_{c_1sc_2} = p_{\bar{c}_1\bar{s}\bar{c}_2} = p_{\bar{c}_2\bar{s}\bar{c}_1} = p_{c_2sc_1}, \qquad q_{c_1sc_2} = q_{\bar{c}_1\bar{s}\bar{c}_2} = t_{\bar{c}_2\bar{s}\bar{c}_1} = t_{c_2sc_1}.$$

It is convenient to combine Propositions 2 and 3 into one theorem.

Theorem 1 (Transformation Theorem). *Given the path* $C_1SC_1[\alpha, \beta](t, p, q)$ *with the lengths of the initial, middle and final segments equal to t, p, and q, respectively, the orthogonal transformations* $\mathcal{G}_{(P_i P_f)}$, $\mathcal{G}_{(O)}$ *and their composition lead to the topologically equivalent paths*

$$C_1SC_2[\alpha, \beta](t, p, q) \simeq \bar{C}_1\bar{S}\bar{C}_2[-\alpha, -\beta](t, p, q) \simeq \bar{C}_2\bar{S}\bar{C}_1[\beta, \alpha](q, p, t) \simeq C_2SC_1[-\beta, -\alpha](q, p, t).$$

The Transformation Theorem gives a linguistic rule for topologically equivalent transformations; it emphasizes the structure of equivalent paths obtained as a result of these transformations. This theorem will be now used for defining equivalency groups and thus reducing the amount of computations, namely the following statement holds.

Proposition 4. *Matrix* $\{a_{ij}\}$ *can be divided into six independent equivalency groups*: (1) $a_{11} \simeq a_{44}$, (2) $a_{12} \simeq a_{21} \simeq a_{34} \simeq a_{43}$, (3) $a_{13} \simeq a_{24} \simeq a_{31} \simeq a_{42}$, (4) $a_{14} \simeq a_{41}$, (5) $a_{22} \simeq a_{33}$, and (6) $a_{23} \simeq a_{32}$.

Indeed, according to the Transformation Theorem, any path with $\alpha \in [0, \pi/2]$, $\beta \in [0, \pi/2, \pi]$ (i.e. belonging to class a_{11}) is transformed into an equivalent path with $\alpha \in [3\pi/2, 2\pi]$, $\beta \in [3\pi/2, 2\pi]$ (which is from class a_{44}). That is, the central symmetry reflection, $\mathcal{G}_{(O)}$, leads to a topologically equivalent path from class a_{11}, while the composition of $\mathcal{G}_{(P_i P_f)}$ and $\mathcal{G}_{(O)}$ leads to a topologically equivalent path from class a_{44}. In the case of the equivalency group (2), for any path of class a_{12} there exists an equivalent path in each of the classes a_{21}, a_{34}, and a_{43}.

By choosing one representative from each equivalency group, we define a *basis set* $\mathcal{B}$ of matrix $\{a_{ij}\}$ — a list of six mutually independent classes of orientation pairs α, β. This reduces from 16 to 6, the number of path classes to be analyzed for the optimal solution. Note that the basis set is not unique since its members can be chosen in various ways.

4. Classes of paths and their equivalency groups

The above scheme for classifying the Dubins set will be fully developed in this section; the necessary analysis involves the following steps:

1. Find the necessary and sufficient condition of non-intersection of the unions $\{C_{il} \cup C_{ir}\}$ and $\{C_{fl} \cup C_{fr}\}$. This condition formally defines what is meant by the "long paths" in the case under study.
2. Show that the condition 1, when satisfied, leads to a further simplification of the set of candidates for the optimal solution that need be considered.

3. For every element of matrix $\{a_{ij}\}$, find the minimum number of the optimal path candidates.
4. For those elements a_{ij} which, as found in step 3, allow more than one candidate for the optimal solution, derive the corresponding *switching functions* which uniquely define the optimal path.

Since elements from the same equivalency group have similar properties, the development steps 3 and 4 are combined below for each of the groups, forming six corresponding subsections.

When applying results of this analysis to a specific problem, one would proceed as follows:

- Make sure that the task at hand satisfies the condition in step 1.
- Associate the given initial and final orientations with a class a_{ij}. For class a_{ij}, use the uniquely defined optimal path.

Below, after analyzing steps 1 and 2, for the sake of convenience we choose for step 3, a particular example of basis set $\mathcal{B}$, $\mathcal{B} = \{a_{11}, a_{12}, a_{13}, a_{14}, a_{22}, a_{23}\}$. For each of the six elements of $\mathcal{B}$, questions posed in steps 3 and 4 are then addressed in the respective six sections.

The following additional notation is used below: unless stated otherwise, forms like AB and $A\breve{}B$ represent straight line segments and circular arc segments, respectively, with A and B being the segments' endpoints. When in mathematical expressions, the same forms denote the lengths of the segments. When needed for clarity, the strings may be longer: e.g. $A_1B_1\breve{}C_1D_1$ is an arc with the endpoints A_1, D_1 and two inner points B_1, C_1.

4.1. The long path case

Turning to the step 1 above, the condition of non-intersection of union $\{C_{il} \cup C_{ir}\}$ with union $\{C_{fl} \cup C_{fr}\}$ is as follows.

Proposition 5. $\{C_{il} \cup C_{ir}\} \cap \{C_{fl} \cup C_{fr}\} = \emptyset$ *if* $d > \sqrt{4 - (|\cos\alpha| + |\cos\beta|)^2} + |\sin\alpha| + |\sin\beta|$. *This condition on d is a precise definition of the long path case.*

To prove this necessary and sufficient condition, consider the case when the union $\{C_{il} \cup C_{ir}\}$ is tangent to the union $\{C_{fl} \cup C_{fr}\}$, i.e. there exist only one point belonging to both unions. Take, for instance, the case a_{11} (α and β are in the first quadrant, Fig. 4). Assume a unit radius, $\rho = 1$. Given a common tangent to both arcs, $IF = IA + AB + BF$. From $\triangle IAO_1$: $IA = \sin\alpha$ and $O_1A = \cos\alpha$. From $\triangle FBO_2$: $BF = \sin\beta$ and $O_2B = \cos\beta$. From $\triangle O_1O_2C$: $O_1O_2 = 2$, $O_2C = O_2B + O_1A$, and therefore $O_1C = \sqrt{4 - (\cos\alpha + \cos\beta)^2}$. Summing up for $IA + AB + BF$, obtain the expression for distance IF, which is a condition for a common tangent for the right initial circle and left final circle. In general, the expression $\sqrt{4 - (|\cos\alpha| + |\cos\beta|)^2} + |\sin\alpha| + |\sin\beta| = d$ covers all possible cases of paths consisting of circular arcs with a common tangent point.

Proposition 6. *For the long path case, the path CCC cannot be the optimal solution.*

To show this, consider the basis set $\mathcal{B}$ of independent orientation pairs (α, β). We need to show that for any element from $\mathcal{B}$, there exists a path of type *CSC* that is shorter than the path *CCC*.

Since for the long path case, $\{C_{il} \cup C_{ir}\} \cap \{C_{fl} \cup C_{fr}\} = \emptyset$, then C_{il}, C_{ir}, C_{fl}, C_{fr} do not intersect. Fig. 5 illustrates this for the general case: it is clear in this example that though the path *CCC* is physically realizable, it can be excluded from the list of candidates for an optimal solution.

To prove this, assume that circle C_{left} is one of the initial circles C_{il} or C_{ir}, and C_{right} is either C_{fl} or C_{fr}. Two other circles tangent to C_{left} and C_{right} are C_{up} (upper tangent) and C_{down} (lower tangent). The initial and final orientations can be chosen either clockwise or counter-clockwise. Notice that the orientation of the initial and final circles has to be the same, since the path of type *CCC* switches directions when passing from one circle to another. If two switchings take place, the initial and final circles must have the same orientation.

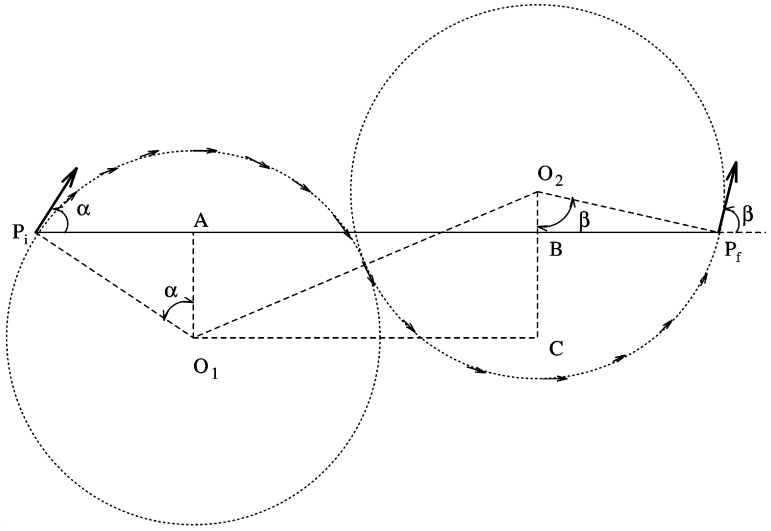

Fig. 4. The case of a path of two circular arcs with a common tangent point; here both orientation angles α and β are in the first quadrant.

The area of possible initial and final positions is limited; the first must lie on the arc $A_1B_1\breve{C}_1D_1$ of circle C_{left}, and the second on the segment $A_2B_2\breve{C}_2D_2$ of circle C_{right} (both segments are shown in solid line in Fig. 5). These restrictions are dictated by Proposition 5.

Let us say, the initial and final positions lie within the arcs $A_1B_1\breve{C}_1D_1$ and $A_2B_2\breve{C}_2D_2$, respectively, both with the same counter-clockwise orientations. (For the clockwise case, the analysis is similar.) There are four options: (i) the initial position $P(t_i)$ belongs to segment $A_1\breve{B}_1C_1$ and the final position $P(t_f)$ to segment $A_2\breve{B}_2C_2$, (ii) $P(t_i) \in C_1\breve{D}_1$ and $P(t_f) \in C_2\breve{D}_2$, (iii) $P(t_i) \in C_1\breve{D}_1$ and $P(t_f) \in A_2\breve{B}_2C_2$, and (iv) $P(t_0) \in A_1\breve{B}_1C_1$ and $P(t_f) \in C_2\breve{D}_2$.

In case (i) the solution *LSL* is the shortest possible path, since the straight line segment connecting C_1 and C_2 is shorter than the sum of segments $C_1\breve{D}_1 + D_1\breve{D}_2 + D_2\breve{C}_2$. In case (ii), the path *LRL* cannot be the optimal solution: since the middle arc is less than $\pi/2$, this path is of type *CCC*, which was shown above to disqualify it from being a

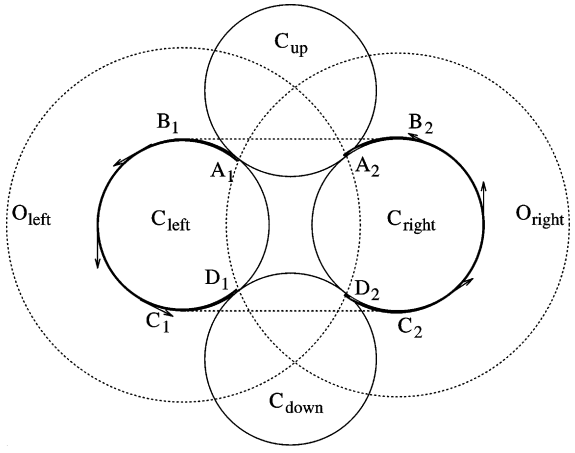

Fig. 5. An illustration to the fact that path *CCC* cannot be the optimal solution in the long path case.

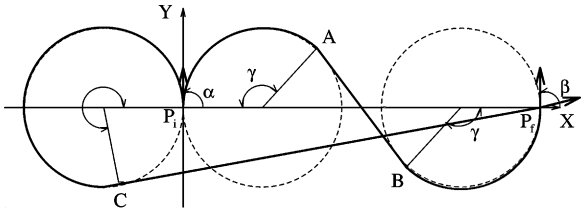

Fig. 6. The optimal solution for class a_{11}; both α and β are in the first quadrant.

candidate for the optimal solution. For the same reason, path *CCC* cannot be the optimal solution in cases (iii) and (iv).

4.2. The equivalency groups of $\{a_{ij}\}$ *classes*

We now turn to defining the equivalency groups for each element of the matrix $\{a_{ij}\}$. Recall that each element represents a class of paths.

4.2.1. Equivalency group $\{a_{11}, a_{44}\}$

According to Proposition 4, classes a_{11} and a_{44} belong to the same equivalency group. We first show for class a_{11} that the corresponding Dubins set can be reduced directly to a unique optimal solution. Then, by applying an orthogonal transformation to the optimal path for class a_{11}, the optimal solution for a_{44} will be obtained.

Proposition 7. *For the long path case* (*see Proposition* 5)*, the optimal solution corresponding to the element* a_{11} *is RSL.*

Note that the number of candidate curves for the optimal path in set $\mathcal{D}$ is now reduced to *LSL*, *LSR*, *RSL*, *RSR*—the curves of type *CCC* are excluded from consideration (Proposition 6). For three of those paths, *LSL*, *LSR*, *RSR*, the x-coordinate goes outside the range $0 \leqslant x \leqslant d$. Take the length of the curve *LS* as the lower bound on the length of the paths *LSL*, *LSR* and *RSR* (*LS* is a subpath of paths *LSL* or *LSR* with $\alpha = \pi/2$).

It is claimed that the upper bound on the length of paths for which the x-coordinate is in the range $0 \leqslant x \leqslant d$ is the path *RSL* with $\alpha = \beta = \pi/2$. Indeed, from Section 2, $\partial\mathcal{L}_{rsl}/\partial\alpha > 0$ and $\partial\mathcal{L}_{rsl}/\partial\beta > 0$. Therefore, the maximum of $\mathcal{L}_{rsl}$ in this region will occur when α and β are equal to $\pi/2$.

To prove that the optimal solution for paths within the range $0 \leqslant x \leqslant d$ is *RSL*, one needs to show that the lower bound on the path length in the Dubins subset {*LSL*, *LSR*, *RSR*} is bigger than the upper bound on the path *RSL*. This case is illustrated in Fig. 6.

Lemma 1. *If* α *and* β *are in the first quadrant then the upper bound for* $\mathcal{L}_{rsl}$ *is limited by*

$$\max_{\alpha,\beta\in[0,\pi/2]} \mathcal{L}_{rsl} \leqslant \sqrt{d^2 - 4d} + 2\pi.$$

Indeed, when $\alpha \in [0, \pi/2]$ and $\beta \in [0, \pi/2]$, the gradient of the path *RSL* is a positive function. This means that the function is monotonically increasing on that interval and reaches its maximum on the interval's boundary, i.e. $\alpha = \beta = \pi/2$. Assuming, as usual, $\rho = 1$, the upper bound for the path length is

$$\mathcal{L}_{rsl} = I\breve{}A + AB + B\breve{}F, \tag{16}$$

where

$$I\breve{}A + B\breve{}F < 2\pi. \tag{17}$$

Segment AB can be found as $AB = 2AD$ or, expressing AD in terms of O_1D and O_1A,

$$AB = 2\sqrt{(\tfrac{1}{2}(d-2))^2 - 1} = \sqrt{d^2 - 4d}. \tag{18}$$

Substituting (17) and (18) into (16), we obtain

$$\max_{\alpha,\beta\in[0,\pi/2]} \mathcal{L}_{rsl} \leqslant \sqrt{d^2 - 4d} + 2\pi.$$

Lemma 2. *If α and β are in the first quadrant then the lower bound on $\mathcal{L}_{lsl}$, $\mathcal{L}_{lsr}$, $\mathcal{L}_{rsr}$ is*

$$\min_{\alpha,\beta\in[0,\pi/2]} \{\mathcal{L}_{lsl}, \mathcal{L}_{lsr}, \mathcal{L}_{rsr}\} \geqslant \sqrt{d^2 + 2d} + 3\pi/2.$$

The lower bound on *LSL*, *LSR* and *RSR* can be obtained by taking $\alpha = \pi/2$ and β as shown in Fig. 6. The minimum path length can then be estimated as

$$\min_{\alpha,\beta\in[0,\pi/2]} \{\mathcal{L}_{lsl}, \mathcal{L}_{lsr}, \mathcal{L}_{rsr}\} = I\breve{E}C + CF > 3\pi/2 + \sqrt{(d+1)^2 - 1} > 3\pi/2 + \sqrt{d^2 + 2d}. \tag{19}$$

In order to prove that the optimal solution corresponding to class a_{11} is *RSL*, we need to show that

$$\min_{\alpha,\beta}\{\mathcal{L}_{lsl}, \mathcal{L}_{lsr}, \mathcal{L}_{rsr}\} - \max_{\alpha,\beta} \mathcal{L}_{rsl} > 0. \tag{20}$$

It is easy to see that (20) holds if $\sqrt{d^2 + 2d} - \sqrt{d^2 - 4d} - \pi/2 > 0$: move $\pi/2$ to the right side of the inequality and multiply both sides by the positive expression $\sqrt{d^2 + 2d} + \sqrt{d^2 - 4d}$. The result is $6d > \pi\sqrt{d^2 + 2d}$, which is true if $d^2 - 4d > 0$ — precisely the case we are interested in. This completes the proof of inequality (20) and of the claim that the optimal solution for class a_{11} is *RSL*. By applying Proposition 2 to the path *RSL*, obtain a similar statement for class a_{44}.

Proposition 8. *Given that a_{11} and a_{44} are in the same equivalency group and the optimal solution for a_{11} is RSL, the optimal solution for a_{44} is LSR.*

4.2.2. Equivalency group $\{a_{12}, a_{21}, a_{34}, a_{43}\}$

According to Proposition 4, path classes $a_{12} \simeq a_{21} \simeq a_{34} \simeq a_{43}$ are in the same equivalency group. We first show how to extract the optimal solution for class a_{12}: it turns out that class a_{12} defines two (rather than one as with class a_{11}) elements of the Dubins set as candidates for the optimal solution. Accordingly, a switching function S_{12} will be derived whose sign will uniquely determine which of the two is the optimal solution. Then, by applying the orthogonal transformation to the paths of class a_{12} (see Proposition 2), optimal solutions for path classes a_{21}, a_{34}, and a_{43} will be obtained.

Proposition 9. *For the long path case, the optimal solution corresponding to the class a_{12} is either RSL or RSR.*

It follows from Proposition 6 that the path of type *CCC* can be excluded from consideration. This leaves four candidates, *RSR*, *RSL*, *LSR*, and *LSL*. Define the *critical initial orientation* as one where orientation α coincides with the tangent to the circle O_{RF}; denote it $\alpha = \bar{\alpha}$. Note that the set (β, d) uniquely defines the critical initial orientation, $\bar{\alpha} = \bar{\alpha}(\beta, d)$. If $\alpha > \bar{\alpha}$ then the path *LSR* is not feasible and can be excluded from consideration; otherwise, path *RSR* should be excluded. Consider the case when path *LSR* is feasible ($\alpha < \bar{\alpha}$). If $\alpha = 0$ and $\beta = \pi$ then the length of *LSR* is equal to that of *RSL*. Analysis of gradients of functions $\mathcal{L}_{rsl}$ and $\mathcal{L}_{lsr}$ shows that if α is increasing or β is decreasing then path *RSL* becomes shorter than *LSR*. This is true until α reaches the critical initial orientation $\alpha = \bar{\alpha}$. Comparing the lower bound on the length of path *LSL* and the upper bound on the length of path

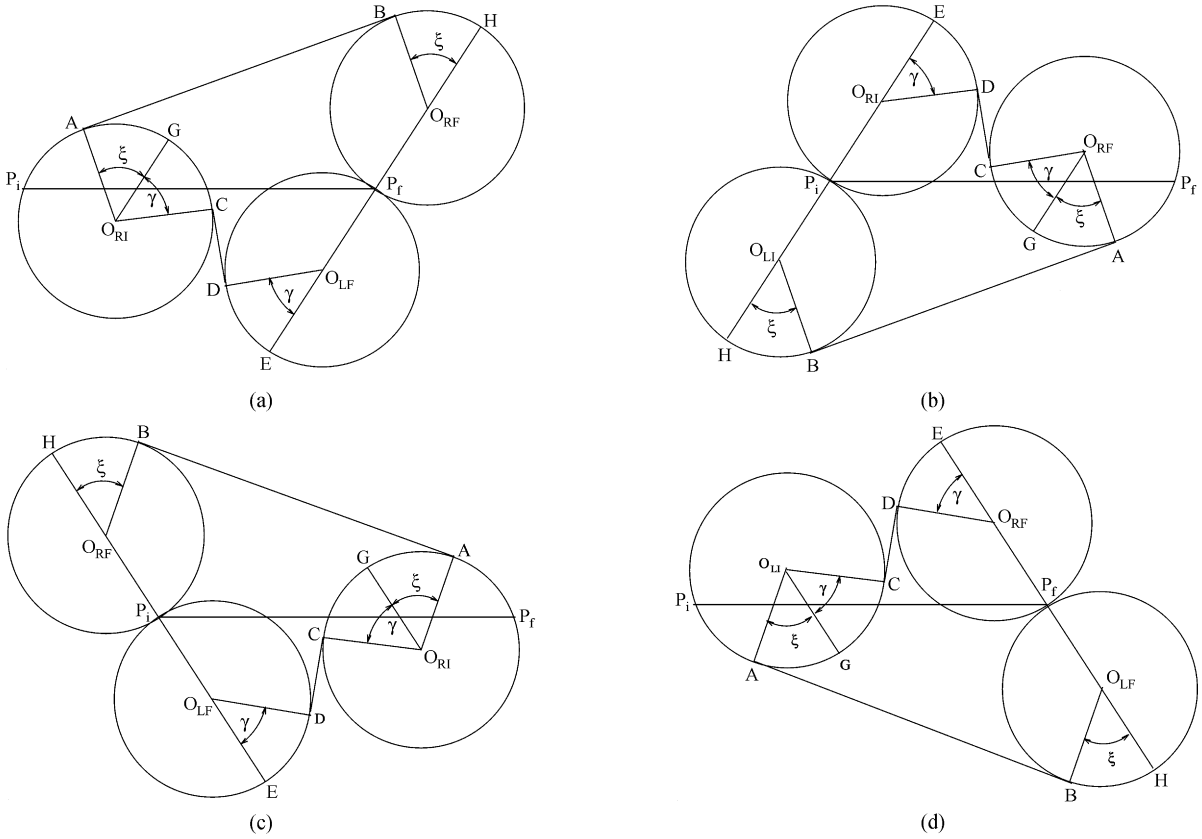

Fig. 7. Choosing the switching functions for the equivalency group $(a_{12}, a_{21}, a_{34}, a_{43})$ — an illustration.

RSL, observe that path *LSL* can be excluded from consideration. This argument plus the fact that $\mathcal{L}_{lsr} > \mathcal{L}_{rsl}$ for $\alpha < \tilde{\alpha}$ end the proof of the proposition.

To find now the optimal solution for class a_{12}, we define a switching function, S_{12}. The following proposition holds.

Proposition 10. *For class* a_{12} (*i.e.* $0 < \alpha \leqslant \pi/2,\ \pi/2 < \beta \leqslant \pi$), *the optimal solution is RSR if* $S_{12}(p_{rsr}, p_{rsl}, q_{rsl}) < 0$, *and it is RSL if* $S_{12}(p_{rsr}, p_{rsl}, q_{rsl}) > 0$, *with*

$$S_{12}(p_{rsr}, p_{rsl}, q_{rsl}) = p_{rsr} - p_{rsl} - 2(q_{rsl} - \pi), \tag{21}$$

where p_{rsr}, p_{rsl}, *and* q_{rsl} *are defined by* (5) *and* (9).

Consider an example in Fig. 7(a); O_{RI}, O_{RF}, and O_{LF} are the centers of circles C_{ri}, C_{rf}, and C_{lf}, respectively. The realizable paths here are *RSR* and *RSL*. Line *EH* connects the origins O_{LF} and O_{RF} and intersects the circles C_{lf} and C_{rf} in points E and H. Since line $O_{RI}G$ is parallel to line *EH*, arc $\breve{AG}$ is equal to arc $\breve{BH}$ defined by the angle ξ, and arc $\breve{GC}$ is equal to arc $\breve{DE}$ defined by the angle γ. For segment *AB*, denote s_{rsr} to be the length of the straight line segment of path *RSR*; similarly for segment *CD*, s_{rsl} is the length of the straight line segment of path *RSL*. Then the path lengths of *RSR* and *RSL* are given by $\mathcal{L}_{rsr} = SA + p_{rsr} + \xi + \pi$ and $\mathcal{L}_{rsl} = SA + \xi + \gamma + p_{rsl} + \gamma + \pi$. Therefore, the sign of the difference $(\mathcal{L}_{rsr} - \mathcal{L}_{rsl})$ defines the bigger of the lengths of *RSR* and *RSL*. Expanding the difference $(\mathcal{L}_{rsr} - \mathcal{L}_{rsl})$ and substituting $\gamma = (q_{rsl} - \pi)$, obtain expression (21) for the switching function of class a_{12}.

Remark. For class a_{12}, the region of α, β where *RSR* is the optimal solution is much smaller than the corresponding region for *RSL*. To save on computations, divide the whole region into two subregions: one where *RSL* is the optimal solution, and the other (much smaller), where the solution is *RSL* or *RSR* and depends on the condition of Proposition 9. The first subregion (where *RSL* is the optimal solution) is defined by

$$d\cos\beta - 3\sin(\beta)\cos\beta + \sin(\beta-\alpha) + \cos\alpha\sin\beta > 0.$$

This case occurs if α and β are such that the last arc in the path *RSL*, q_{rsl}, is equal to π. If $q_{rsl} < \pi$ then path *RSL* is shorter than path *RSR*. If $q_{rsl} > \pi$, then the switching function S_{12} needs be checked.

We now turn to the classes a_{21}, a_{34}, and a_{43} which are in the same equivalency group as a_{12}. By applying the orthogonal transformation (see Proposition 2), the set of path candidates for a_{12} is transformed into the set of candidates for the remaining elements of the equivalency group a_{21}, a_{34}, a_{43} (see Fig. 7). That leads to the following result.

Proposition 11. *Since $a_{12} \simeq a_{21} \simeq a_{34} \simeq a_{43}$ and the optimal solution for a_{12} is {RSL or RSR}, then the optimal solutions for the remaining elements of this equivalency group are $a_{21} \mapsto$ {RSL or LSL}; $a_{34} \mapsto$ {LSR or RSR}; $a_{43} \mapsto$ {LSR or LSL}.*

The respective switching functions for classes a_{21}, a_{34}, and a_{43} (see the next three propositions) are obtained from the switching function for class a_{12}, by replacing t and q segments as prescribed by the transformation theorem.

Proposition 12. *For class a_{21} (i.e. $\pi/2 < \alpha \leqslant \pi,\ 0 < \beta \leqslant \pi/2$), the optimal solution is LSL if $S_{21} < 0$, and it is RSL if $S_{21} > 0$, with*

$$S_{21}(p_{lsl}, p_{rsl}, t_{rsl}) = p_{lsl} - p_{rsl} - 2(t_{rsl} - \pi). \tag{22}$$

To check, apply Theorem 1 to the switching function $S_{12} = \mathcal{L}_{rsr} - \mathcal{L}_{rsl} = p_{rsr} - p_{rsl} - 2\gamma$, where $\gamma = q_{rsl} - \pi$; obtain $\mathcal{L}_{rsr} = SA + p_{rsr} + \xi + \pi$ and $\mathcal{L}_{rsl} = SA + \xi + \gamma + p_{rsr} + \gamma + \pi$. According to Proposition 3, the orthogonal transformation implies

$$\mathcal{L}_{rsr}(\alpha \in [0,\pi/2], \beta \in [\pi/2,\pi]) = \mathcal{L}_{lsl}(\alpha \in [\pi/2,\pi], \beta \in [0,\pi/2]),$$

and, additionally, $p_{rsr}(\alpha \in [0,\pi/2], \beta \in [\pi/2,\pi]) = p_{lsl}(\alpha \in \alpha \in [\pi/2,\pi], \beta \in [0,\pi/2])$ and $p_{rsl}(\alpha \in [0,\pi/2], \beta \in [\pi/2,\pi]) = p_{rsl}(\alpha \in \alpha \in [\pi/2,\pi], \beta \in [0,\pi/2])$, and $q_{rsl}(\alpha \in [0,\pi/2], \beta \in [\pi/2,\pi]) = t_{rsl}(\alpha \in \alpha \in [\pi/2,\pi], \beta \in [0,\pi/2])$. The switching function for class a_{21} can be simply obtained from the function S_{12} by changing the segments from $p_{rsr}, p_{rsl}, q_{rsl}$ to $p_{lsl}, p_{rsl}, t_{rsl}$, respectively. The validity of this procedure follows from the transformation theorem, and using again the same theorem, obtain directly the switching functions for classes a_{34} and a_{43}.

Proposition 13. *For class a_{34} (i.e. $\pi < \alpha \leqslant 3\pi/2,\ 3\pi/2 < \beta \leqslant 2\pi$), the optimal solution is RSR if $S_{34} < 0$, and it is LSR if $S_{34} > 0$, with*

$$S_{34}(p_{rsr}, p_{lsr}, t_{lsr}) = p_{rsr} - p_{lsr} - 2(t_{lsr} - \pi). \tag{23}$$

Proposition 14. *For class a_{43} (i.e. $3\pi/2 < \alpha \leqslant 2\pi,\ \pi < \beta \leqslant 3\pi/2$), the optimal solution is LSL if $S_{43} < 0$, and it is LSR if $S_{43} > 0$, with*

$$S_{43}(p_{lsl}, p_{lsr}, q_{lsr}) = p_{lsl} - p_{lsr} - 2(q_{lsr} - \pi). \tag{24}$$

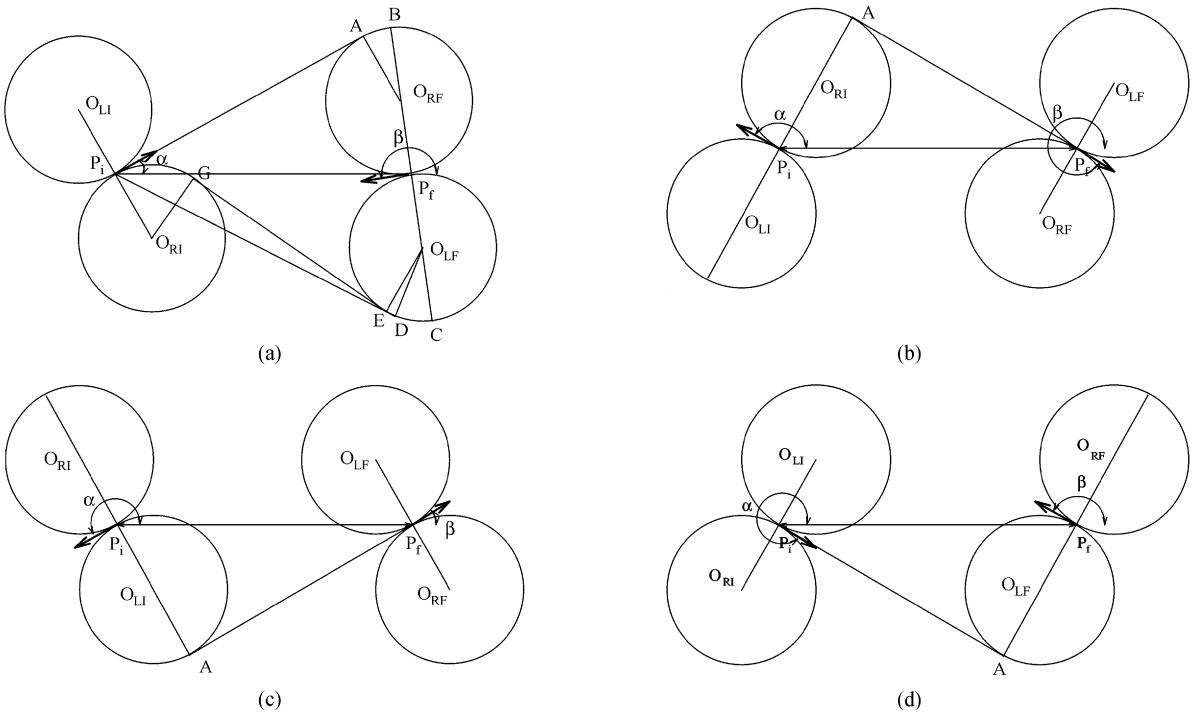

Fig. 8. Choosing the switching functions for the equivalency group $(a_{13}, a_{24}, a_{31}, a_{42})$ — an illustration.

4.2.3. Equivalency group $\{a_{13}, a_{24}, a_{31}, a_{42}\}$

According to Proposition 4, classes $a_{13}, a_{24}, a_{31}, a_{42}$ belong to the same equivalency group. First we show that for class a_{13} the Dubins set can be reduced to two path candidates, and then further reduced to a unique optimal solution using an appropriate switching function, S_{13}. Then, by applying the transformation theorem, the switching function S_{13} will be modified to produce the corresponding switching functions for classes a_{24}, a_{31}, a_{42}. For a_{13}, the following holds.

Proposition 15. *For the long path case, the optimal solution corresponding to the element* a_{13} *is either RSR or LSR.*

Similar to the argument for class a_{12} above, one can see that path *RSL* can be excluded from the set of candidates considered for the optimal path. Indeed, if $\alpha = 0$ and $\beta = \pi$, then $\mathcal{L}_{lsr} = \mathcal{L}_{rsl}$. If α or β are increasing then path *LSR* becomes shorter than path *RSL*. To see this, compare the line segment *SD*, which is a tangent to circle O_{LF}, with *SD*, a tangent to circle O_{RF} (see Fig. 8(a)). Now, $SA < SD$ for any $\beta \in (\pi, 3\pi/2]$, and $A\breve{}B < D\breve{}C$; also, $SD < S\breve{}G + GE + E\breve{}D$. This leads to

$$SA + A\breve{}B < S\breve{}G + GE + E\breve{}C.$$

Therefore, if $\alpha \in [0, \bar{\alpha}]$ then $\mathcal{L}_{lsr} < \mathcal{L}_{rsl}$. Similarly, if $\alpha > \bar{\alpha}$ then $\mathcal{L}_{rsr} < \mathcal{L}_{rsl}$. Here $\bar{\alpha}$ is the critical angle $\alpha = \bar{\alpha}(d, \beta)$, where paths *LSR* and *RSR* degenerate to *SR*. This implies that only paths *LSR* and *RSR* are candidates for the optimal solution.

Using Proposition 2, a similar argument extends this result to the remaining three elements, as follows.

Proposition 16. *Since $a_{13} \simeq a_{24} \simeq a_{31} \simeq a_{42}$ and the optimal solution for a_{13} is either RSR or LSR, the optimal solutions for a_{24}, a_{31}, a_{42} are, respectively,*

$$a_{24} \mapsto \{RSR \text{ or } RSL\};\ a_{31} \mapsto \{LSL \text{ or } LSR\};\ a_{42} \mapsto \{LSL \text{ or } RSL\}.$$

Turning back to class a_{13}, we can verify that the critical angle $\bar{\alpha}$ defines switching of the optimal path from *LSR* to *RSR*; i.e. if $\alpha > \bar{\alpha}$ the optimal solution is *RSR*, otherwise it is *LSR*. Another indicator of the switch from *LSR* to *RSR* is the length of arc t_{rsr}. Notice that if *RSR* is the optimal solution for class a_{13} then t_{rsr} cannot exceed π.

This observation leads to the corresponding switching functions necessary for obtaining the optimal solution.

Proposition 17. *For class a_{13} (i.e. $0 < \alpha \leqslant \pi/2,\ 3\pi/2 < \beta \leqslant 2\pi$), if*

1. *$S_{13}(t_{rsr}) < 0$, then the optimal solution is RSR,*
2. *$S_{13}(t_{rsr}) > 0$, then the optimal solution is LSR,*

where

$$S_{13}(t_{rsr}) = t_{rsr} - \pi. \tag{25}$$

The transformation theorem extends the results obtained for class a_{13} to the accompanying classes a_{24}, a_{31} and a_{42}.

Proposition 18. *For class a_{24} (i.e. $\pi/2 < \alpha \leqslant \pi,\ 3\pi/2 < \beta \leqslant 2\pi$), the optimal solution is RSR if $S_{24} < 0$, and it is RSL otherwise, where*

$$S_{24}(q_{rsr}) = q_{rsr} - \pi. \tag{26}$$

Proposition 19. *For class a_{31} (i.e. $\pi < \alpha \leqslant 3\pi/2,\ 0 < \beta \leqslant \pi/2$), the optimal solution is LSL if $S_{31} < 0$, and it is LSR otherwise, where*

$$S_{31}(q_{lsl}) = q_{lsl} - \pi. \tag{27}$$

Proposition 20. *For class a_{42} (i.e. $3\pi/2 < \alpha \leqslant 2\pi,\ \pi/2 < \beta \leqslant \pi$), the optimal solution is RSL if $S_{42} < 0$, and it is LSL otherwise, where*

$$S_{42}(t_{lsl}) = t_{lsl} - \pi. \tag{28}$$

4.2.4. Equivalency group $\{a_{14}, a_{41}\}$

According to Proposition 4, path classes $a_{14} \simeq a_{41}$ are in the same equivalency group, and so, by the rules established in the transformation theorem, the classification of optimal solutions for class a_{14} leads to the optimal solutions for class a_{41}.

Proposition 21. *For the long path case, the optimal solution corresponding to the element a_{14} is {RSR or LSR or RSL}.*

Recall that by now the total number of candidates for the optimal solution is reduced to four — *LSL*, *LSR*, *RSL*, *RSR* — because the curves of type *CCC* are excluded from consideration due to Proposition 4. As before, define the critical orientations, which for class a_{14} appear for both α and β (see Fig. 9): namely, the values d and β determine the critical orientation for α, $\bar{\alpha} = \bar{\alpha}(d, \beta)$, and the values d and α determine the critical orientation for β, $\bar{\beta} = \bar{\beta}(d, \alpha)$ (notice that $\bar{\alpha} \neq \alpha(d, \bar{\beta})$).

Among the four path candidates mentioned, path *LSL* can be excluded from consideration since the lower bound for this path is bigger than the upper bound for path *RSR*. The critical angle $\bar{\alpha}$ gives the optimal solution *SR*, and

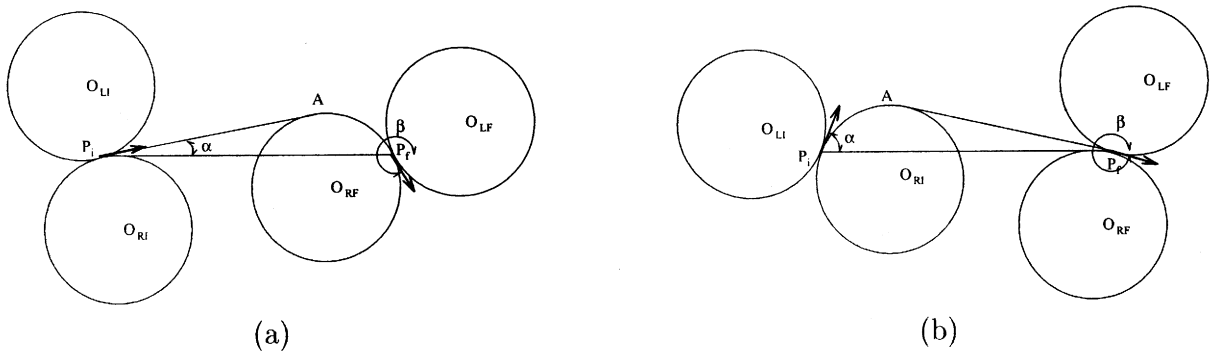

Fig. 9. Example of critical orientations of the path candidates for class a_{14}.

thus defines the switch condition for the optimal path from *LSR* to *RSR*. Similarly, the critical angle $\bar{\beta}$ indicates the switch of the optimal path from *RSR* to *RSL*.

The proof of these facts is similar to those for classes a_{11} and a_{13}. Define two critical angles: $\alpha = \bar{\alpha}(d, \beta)$ — the angle at which paths *LSR* and *RSR* degenerate into the path *SR*, and $\beta = \bar{\beta}(d, \alpha)$ — the angle at which paths *RSR* and *RSL* degenerate into the path *RS*. First consider the case when $\alpha \in [\bar{\alpha}, \pi/2]$ and $\beta \in [3\pi/2, \beta(d, \bar{\alpha})]$. It is claimed that if $\alpha \in [\bar{\alpha}, \pi/2]$ and $\beta \in [3\pi/2, \beta(d, \bar{\alpha})]$ then the upper bound for $\mathcal{L}_{rsr}$ is limited by

$$\max_{\alpha\in[\bar{\alpha},\pi/2],\beta\in[3\pi/2,\beta(d,\bar{\alpha})]} \mathcal{L}_{rsr} \leqslant d - 2 + \pi.$$

Indeed, the gradient of $\mathcal{L}_{rsr}$ is strictly positive when $\alpha \in [\bar{\alpha}, \pi/2]$ and strictly negative when $\beta \in [3\pi/2, \bar{\beta}]$. In the regions $\alpha \in [\bar{\alpha}, \pi/2]$ and $\beta \in [3\pi/2, \bar{\beta}]$, the maximum length of path *RSR* occurs when $\alpha = \pi/2$ and $\beta = 3\pi/2$ (this follows from monotonicity of the function $\mathcal{L}_{rsr}$), i.e. when

$$\max_{\alpha\in[\bar{\alpha},\pi/2],\beta\in[\bar{\beta},2\pi]} \mathcal{L}_{rsr} \leqslant d - 2 + \pi. \tag{29}$$

One can conclude that if $\alpha \in [\bar{\alpha}, \pi/2]$ and $\beta \in [3\pi/2, \bar{\beta}]$ then the lower bound on $\mathcal{L}_{lsl}$, $\mathcal{L}_{rsl}$, and $\mathcal{L}_{lsr}$ is

$$\min_{\alpha\in[\bar{\alpha},\pi/2],\beta\in[3\pi/2,\bar{\beta}]} \{\mathcal{L}_{lsl}, \mathcal{L}_{rsl}, \mathcal{L}_{lsr}\} \geqslant \sqrt{d^2 + 2d} + 3\pi/2.$$

These critical cases are shown in Fig. 10. The resulting bounds are

$$\min_{\alpha\in[\bar{\alpha},\pi/2],\beta\in[3\pi/2,\bar{\beta}]} \mathcal{L}_{lsl} \geqslant 3\pi + d + 2, \tag{30}$$

$$\min_{\alpha\in[\bar{\alpha},\pi/2],\beta\in[3\pi/2,\bar{\beta}]} \mathcal{L}_{rsl} \geqslant 3\pi/2 + \sqrt{d^2 + 2d}, \tag{31}$$

$$\min_{\alpha\in[\bar{\alpha},\pi/2],\beta\in[3\pi/2,\bar{\beta}]} \mathcal{L}_{lsr} \geqslant 3\pi/2 + \sqrt{d^2 + 2d}. \tag{32}$$

This leads to the condition

$$\min_{\alpha\in[\bar{\alpha},\pi/2],\beta\in[3\pi/2,\bar{\beta}]} \{\mathcal{L}_{lsl}, \mathcal{L}_{rsl}, \mathcal{L}_{lsr}\} \geqslant 3\pi/2 + \sqrt{d^2 + 2d}. \tag{33}$$

Notice that the lower bound on paths $\{\mathcal{L}_{lsl}, \mathcal{L}_{rsl}, \mathcal{L}_{lsr}\}$ is larger than the upper bound on $\mathcal{L}_{rsr}$ (Eqs. (29) and (33)). This completes the proof of the fact that if $\alpha \in [\bar{\alpha}, \pi/2]$ and $\beta \in [3\pi/2, \beta(d, \bar{\alpha})]$, then the path *RSR* is the optimal

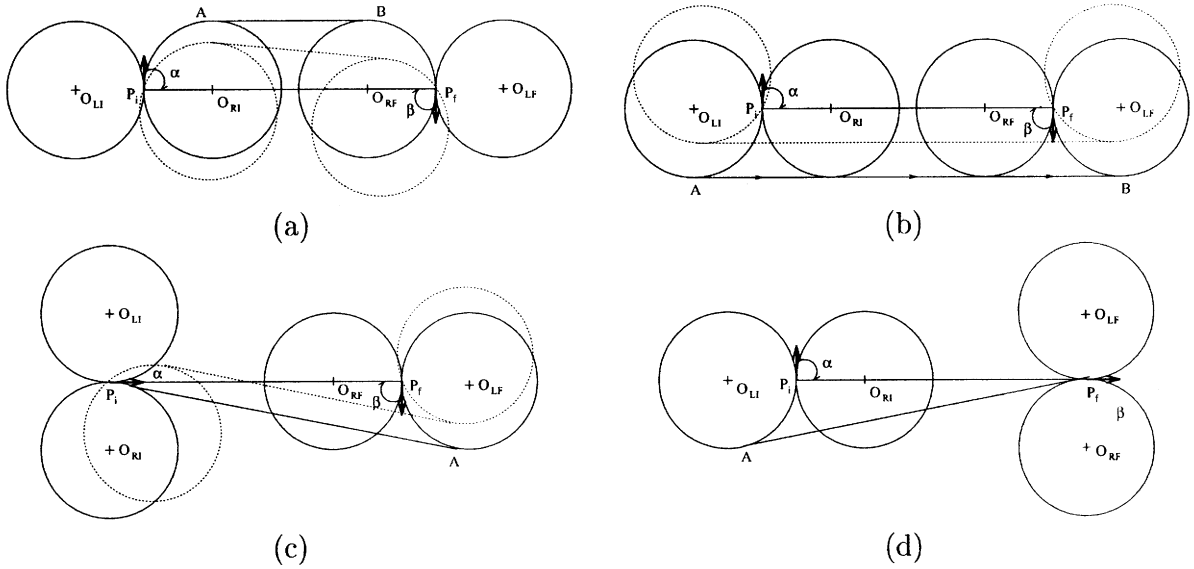

Fig. 10. Example of critical orientations of the path candidates for class a_{14}.

solution. For class a_{14} two more candidates are possible, i.e. *LSR* and *RSL*. The proposition below relates the set of candidates for class a_{14} to the accompanying class a_{41}.

Proposition 22. *Since $a_{14} \simeq a_{41}$ and the optimal solution for class a_{14} is {LSR or RSL or RSR}, the optimal solution for class a_{41} is {RSL or LSR or LSL}.*

Similar to the class a_{13}, the critical angles $\bar{\alpha}$ and $\bar{\beta}$ define the switch of the optimal solution from *RSR* to *LSR* and from *RSR* to *RSL*, respectively. To simplify the calculations, we choose to build our classification based on the length of segments t_{rsr} and q_{rsr}. Following the same logic as in the case of class a_{13}, one notices that t_{rsr} and q_{rsr} cannot exceed π if *RSR* is an optimal solution for class a_{14}. If either of the two segments t_{rsr} or q_{rsr} is bigger than π, then there is always another path that is shorter than *RSR*; i.e. if $t_{rsr} > \pi$ then the optimal solution is *LSR*, and if $q_{rsr} > \pi$ then the optimal solution is *RSL*. This observation leads to the following classification rule.

Proposition 23. *For class a_{14} (i.e. $0 < \alpha \leqslant \pi/2,\ 3\pi/2 < \beta \leqslant 2\pi$), if*

1. $S^1_{14}(t_{rsr}) > 0$, *then the optimal solution is RSR,*
2. $S^2_{14}(q_{rsr}) > 0$, *then the optimal solution is RSL,*
3. *if neither* (1) *or* (2) *holds, then the optimal solution is RSR,*

where

$$S^1_{14}(t_{rsr}) = t_{rsr} - \pi, \tag{34}$$

$$S^2_{14}(t_{rsr}) = q_{rsr} - \pi. \tag{35}$$

By applying the transformation theorem, obtain the switching conditions for class a_{41}.

Proposition 24. *For class a_{41} (i.e. $3\pi/2 < \alpha \leqslant 2\pi,\ 0 < \beta \leqslant \pi/2$), if*

1. $S^1_{41}(t_{rsr}) > 0$, *then the optimal solution is RSL,*

2. $S_{14}^2(q_{rsr}) > 0$, *then the optimal solution is LSR,*
3. *if neither* (1) *or* (2) *holds, then the optimal solution is LSL,*

where

$$S_{14}^1(t_{lsl}) = t_{lsl} - \pi, \tag{36}$$

$$S_{14}^2(t_{lsl}) = q_{lsl} - \pi. \tag{37}$$

4.2.5. Equivalency group $\{a_{22}, a_{33}\}$

According to Proposition 4, classes $a_{22} \simeq a_{33}$ are in the same equivalency group, and so the classification of optimal solutions for class a_{22} leads to that for class a_{33}.

Proposition 25. *For the long path case, the optimal solution corresponding to the class* a_{22} *is* {*LSL or RSL or RSR*}.

The path *LSR* is excluded from the consideration since $\mathcal{L}_{lsr}$ is always larger than $\mathcal{L}_{rsl}$. Indeed, for $\alpha = \beta = \pi$ the lengths $\mathcal{L}_{lsr} = \mathcal{L}_{rsl}$, and path *LSR* has its minimum at $\alpha = \beta = \pi$, and path *RSL* — its maximum within class a_{22}.

Proposition 26. *Since* $a_{22} \simeq a_{33}$ *and the optimal solution for* a_{22} *is* {*LSL or* {*RSL or RSR*}}, *then the optimal solution for* a_{33} *is* {*RSR or* {*LSR or LSL*}}.

The following proposition gives the condition for finding the optimal paths.

Proposition 27. *For class* a_{22} (*i.e.* $\pi/2 < \alpha \leqslant \pi,\ \pi/2 < \beta \leqslant \pi$), *if*

1. $\alpha > \beta$ *and* $S_{22}^1 < 0$, *the optimal solution is LSL,*
2. $\alpha > \beta$ *and* $S_{22}^1 > 0$, *the optimal solution is RSL,*
3. $\alpha < \beta$ *and* $S_{22}^2 < 0$, *the optimal solution is RSR,*
4. $\alpha < \beta$ *and* $S_{22}^2 > 0$, *the optimal solution is RSL,*

where the switching functions are

$$S_{22}^1(p_{lsl}, p_{rsl}, t_{rsl}) = p_{lsl} - p_{rsl} - 2(t_{rsl} - \pi), \tag{38}$$

$$S_{22}^2(p_{rsr}, p_{rsl}, q_{rsl}) = p_{rsr} - p_{rsl} - 2(q_{rsl} - \pi), \tag{39}$$

and p_{lsl}, p_{rsr}, p_{rsl}, t_{rsl}, *and* q_{rsl} *are defined by* (3) *and* (9), *respectively.*

The proof of the proposition is similar to that for class a_{12} with the only difference that the set of candidates depends upon the relations between α and β. Notice that if $\alpha = \beta$ then the length of path *LSL* is equal to that of *RSR*. When α starts increasing, path *LSL* becomes shorter than path *RSR* (see Fig. 11). Similarly, using the transformation theorem, obtain the solutions for class a_{33} are as follows.

Proposition 28. *For class* a_{33} (*i.e.* $\pi < \alpha \leqslant 3\pi/2,\ \pi < \beta \leqslant 3\pi/2$), *if*

1. $\alpha < \beta$ *and* $S_{33}^1 < 0$, *the optimal solution is RSR,*
2. $\alpha > \beta$ *and* $S_{33}^1 > 0$, *the optimal solution is LSR,*
3. $\alpha < \beta$ *and* $S_{33}^2 < 0$, *the optimal solution is LSL,*
4. $\alpha > \beta$ *and* $S_{33}^2 > 0$, *the optimal solution is LSR,*

where the switching functions are

$$S_{33}^1(p_{rsr}, p_{lsr}, t_{lsr}) = p_{rsr} - p_{lsr} - 2(t_{lsr} - \pi), \tag{40}$$

$$S_{33}^2(p_{lsl}, p_{lsr}, q_{lsr}) = p_{lsl} - p_{lsr} - 2(q_{lsr} - \pi). \tag{41}$$

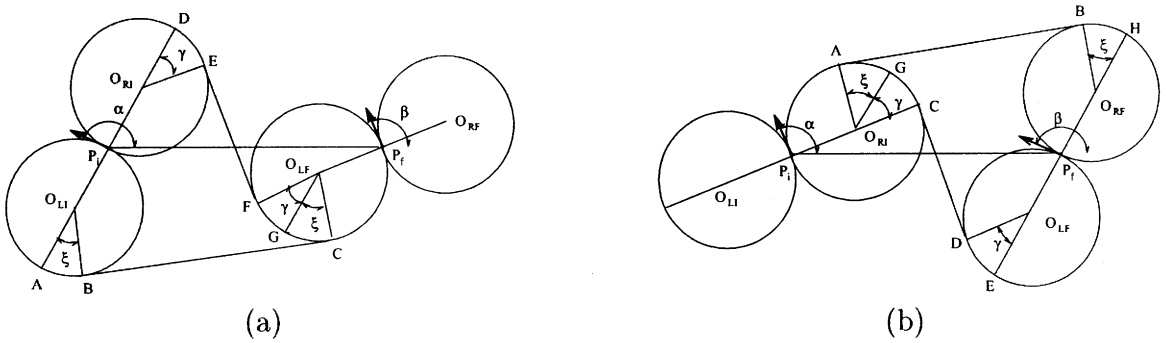

Fig. 11. For class a_{22}, the set of candidates for the optimal solution depends much upon the relations between α and β: if $\alpha > \beta$, the candidates are *LSL* and *RSL*, otherwise they are *RSR* and *RSL*.

4.2.6. Equivalency group $\{a_{23}, a_{32}\}$

According to Proposition 4, classes $a_{23} \simeq a_{32}$ are in the same equivalency group. The corresponding classification of optimal solutions proceeds as follows.

Proposition 29. *For the long path case, the optimal solution corresponding to the class* a_{23} *is RSR.*

Four path candidates need be considered here — *RSR*, *RSL*, *LSR*, *LSL*. Note that

$$\max_{\alpha\in[\pi/2,\pi],\beta\in[\pi,3\pi/2]} \mathcal{L}_{rsr} = \min_{\alpha\in[\pi/2,\pi],\beta\in[\pi,3\pi/2]} \{\mathcal{L}_{rsl}\mathcal{L}_{lsr}\mathcal{L}_{lsl}\}.$$

The maximum of the length of path *RSR* and the minimum of $\{\mathcal{L}_{rsl}\mathcal{L}_{lsr}\mathcal{L}_{lsl}\}$ occur when $\alpha = \beta = \pi$. By applying the transformation theorem, the classification for a_{32} is given by the following proposition.

Proposition 30. *Since* $a_{23} \simeq a_{32}$ *and the optimal solution for* a_{23} *is RSR, the optimal solution for* a_{32} *is LSL.*

The switching functions are logical functions of Boolean type. They are not uniquely defined. The choice of a particular function will be usually guided by computational considerations.

5. The main result

We can now summarize the whole scheme developed above, which presents the main result of this work. Using the scheme, the problem of finding the shortest smooth path between two configurations is solved without an explicit calculation of the paths involved. Instead, a simple logical scheme is used based on the aggregation of all possible paths into classes a_{ij} and on the equivalency groups as defined above.

The input to the scheme are the angular quadrants of the directional angles (α, β); its output is the name of the element of the Dubins set that presents the shortest path. The scheme forms a decision tree summarized in the table in Fig. 12. Each block of the table represents one element a_{ij} of matrix $\{a_{ij}\}$ and includes the corresponding options for the optimal path. It may take only one step to obtain the solution, as e.g. the solution *RSL* for the quadrants (1, 1), or it may take two steps, as for the quadrants (3, 1), or it may take at most three steps, as for the quadrants (2, 2) (Fig. 12). When the second and third steps are necessary, their outcome is determined by the signs of one or two *switching functions* $\{S\}$. The general form of functions $\{S\}$ is

$$f(s_1, s_2, s_3) = s_1 - s_2 - 2(s_3 - \pi), \qquad g(s) = s - \pi. \tag{42}$$

Initial Quadrant \ Final Quadrant	1	2	3	4
1	RSL	if $S_{12} < 0$ then RSR if $S_{12} > 0$ then RSL	if $S_{13} < 0$ then RSR if $S_{13} > 0$ then LSR	if $S^1_{14} > 0$ then LSR if $S^2_{14} > 0$ then RSL else RSR
2	if $S_{21} < 0$ then LSL if $S_{21} > 0$ then RSL	if $S^1_{22} < 0$ then LSL if $S^1_{22} > 0$ then RSL if $S^2_{22} < 0$ then RSR if $S^2_{22} > 0$ then RSL	RSR	if $S_{24} < 0$ then RSR if $S_{24} > 0$ then RSL
3	if $S_{31} < 0$ then LSL if $S_{31} > 0$ then LSR	LSL	if $S^1_{33} < 0$ then RSR if $S^1_{33} > 0$ then LSR if $S^2_{33} < 0$ then LSL if $S^2_{33} > 0$ then LSR	if $S_{34} < 0$ then RSR if $S_{34} > 0$ then LSR
4	if $S^1_{41} > 0$ then RSL if $S^2_{41} > 0$ then LSR else LSL	if $S_{42} < 0$ then LSL if $S_{42} > 0$ then RSL	if $S_{43} < 0$ then LSL if $S_{43} > 0$ then LSR	LSR

Fig. 12. The decision table for finding the shortest path.

The complete list of switching functions for all classes a_{ij} is as follows (note that for some classes, the unique optimal solution is obtained directly, without switching functions):

$$
\begin{aligned}
&\text{Class } a_{11}: \quad \text{unique solution},\\
&\text{Class } a_{12}: \quad S_{12} = f(p_{rsr}, p_{rsl}, q_{rsl}) = p_{rsr} - p_{rsl} - 2(q_{rsl} - \pi),\\
&\text{Class } a_{13}: \quad S_{13} = g(t_{rsr}) = t_{rsr} - \pi,\\
&\text{Class } a_{14}: \quad S^1_{14} = g(t_{rsr}) = t_{rsr} - \pi, \qquad S^2_{14} = g(q_{rsr}) = q_{rsr} - \pi,\\
&\text{Class } a_{21}: \quad S_{21} = f(p_{lsl}, p_{rsl}, t_{rsl}) = p_{lsl} - p_{rsl} - 2(t_{rsl} - \pi),\\
&\text{Class } a_{22}: \quad \begin{cases} \text{if } \alpha > \beta, \text{ then } S^1_{22} = f(p_{lsl}, p_{rsl}, t_{rsl}) = p_{lsl} - p_{rsl} - 2(t_{rsl} - \pi),\\ \text{if } \alpha < \beta, \text{ then } S^2_{22} = f(p_{rsr}, p_{rsl}, q_{rsl}) = p_{rsr} - p_{rsl} - 2(q_{rsl} - \pi), \end{cases}\\
&\text{Class } a_{23}: \quad \text{unique solution},\\
&\text{Class } a_{24}: \quad S_{24} = g(q_{rsr}) = q_{rsr} - \pi,\\
&\text{Class } a_{31}: \quad S_{31} = g(q_{lsl}) = q_{lsl} - \pi,\\
&\text{Class } a_{32}: \quad \text{unique solution},\\
&\text{Class } a_{33}: \quad \begin{cases} \text{if } \alpha < \beta, \text{ then } S^1_{33} = f(p_{rsr}, p_{lsr}, t_{lsr}) = p_{rsr} - p_{lsr} - 2(t_{lsr} - \pi),\\ \text{if } \alpha > \beta, \text{ then } S^2_{33} = f(p_{lsl}, p_{lsr}, q_{lsr}) = p_{lsl} - p_{lsr} - 2(q_{lsr} - \pi), \end{cases}\\
&\text{Class } a_{34}: \quad S_{34} = f(p_{rsr}, p_{lsr}, t_{lsr}) = p_{rsr} - p_{lsr} - 2(t_{lsr} - \pi),\\
&\text{Class } a_{41}: \quad S^1_{41} = g(t_{lsl}) = t_{lsl} - \pi, \qquad S^2_{41} = g(q_{lsl}) = q_{lsl} - \pi,\\
&\text{Class } a_{42}: \quad S_{42} = g(t_{lsl}) = t_{lsl} - \pi,\\
&\text{Class } a_{43}: \quad S_{43} = f(p_{lsl}, p_{lsr}, q_{lsr}) = p_{lsl} - p_{lsr} - 2(q_{lsr} - \pi),\\
&\text{Class } a_{44}: \quad \text{unique solution}.
\end{aligned}
\tag{43}
$$

Take, e.g. a set ($\alpha \in [0, \pi/2], \beta \in [\pi/2, \pi]$), which corresponds to the element a_{12} of matrix $\{a_{ij}\}$. Block (1, 2) in the table in Fig. 12 suggests that the optimal solution is either *RSL* or *RSR*. The switching function S_{12} listed in block (1, 2) is then calculated as in the list above (Eq. (42)); its elements p_{rsr}, p_{rsl} and q_{rsl} come from the second equation of (5) and the second and third equations of (9), respectively. The sign of S_{12} then determines which of the two versions indicated in block (1, 2) is the unique solution.

To demonstrate efficiency of the proposed classification scheme, consider the task of finding the shortest smooth path from P_i to P_f, located on the distance $|P_i P_f| = 6$, such that the path starts and ends with the directions of motion $\alpha = \pi/6$ and $\beta = \pi/3$, respectively, and the path radius of curvature is limited by $\rho = 1$. According to Dubins result, six paths candidates {*LSL*, *RSR*, *RSL*, *LSR*, *RLR*, *LRL*} have to be calculated and compared. Using expressions given in Section 2

$$\begin{aligned}
&\mathcal{L}_{lsl} = t_{lsl} + p_{lsl} + q_{lsl} = -\alpha + \beta + p_{lsl} = 12.4526,\\
&\mathcal{L}_{rsr} = t_{rsr} + p_{rsr} + q_{rsr} = \alpha - \beta + p_{rsr} = 12.1361,\\
&\mathcal{L}_{lsr} = t_{lsr} + p_{lsr} + q_{lsr} = \alpha - \beta + 2t_{lsr} + p_{lsr} = 18.3890,\\
&\mathcal{L}_{rsl} = t_{rsl} + p_{rsl} + q_{rsl} = -\alpha + \beta + 2t_{rsl} + p_{rsl} = 6.2488,\\
&\mathcal{L}_{rlr} = t_{rlr} + p_{rlr} + q_{rlr} = \alpha - \beta + 2p_{rlr} \quad \text{path is not feasible},\\
&\mathcal{L}_{lrl} = t_{lrl} + p_{lrl} + q_{lrl} = -\alpha + \beta + 2p_{lrl} \quad \text{path is not feasible}.
\end{aligned} \tag{44}$$

After all paths-candidates are calculated and compared, we conclude that the shortest path is *RSL*. In contrast, if we use the approach proposed in this paper, then based only on information about the initial and final configuration and without any calculations involved, we can make the same conclusion. Indeed, for the case studied, the initial and final configurations are in the first quadrant, i.e. the path belongs to the class a_{11}. According to the look-up table (Fig. 12), the optimal solution for all paths from this class have to have the topology *RSL*. Thus, using the classification scheme we were able to obtain the optimal solution without any calculations involved. This example is a good illustration of the computational efficiency of the proposed classification scheme.

6. Conclusion

The central idea developed in this work is that the problem of finding the shortest path between two configurations can be reduced to a logical manipulation of the set of appropriate path candidates, without their explicit calculation. This is in sharp departure from the direct computation and comparison of the candidate paths that the existing techniques require. The candidate paths come from the sufficient set known as the Dubins set [5]. One direct benefit of the suggested scheme is computational savings — an important consideration in real-time control. For example, when attempting to find the shortest path to a given position/orientation (configuration) for a driverless car or a mobile robot, one would simply find in the table (Fig. 12), the element that corresponds to the initial and final configurations, and then pinpoint the unique solution either immediately or using the sign of an appropriate switching function of the form (42).

As mentioned in Section 1, the derivation of the approach is simplified if the problem at hand is divided into two cases, called here the *long path case* and the *short path case*. To save space, the suggested logical classification scheme is fully developed here only for the long path case. Situations with short paths require a roughly similar, though a bit tedious, analysis, resulting in a computational procedure that is somewhat more complex and less economical than the one presented here (see Proposition 5 for a formal definition of both cases).

The presented result also gives a new interesting insight into the nature of Dubins' problem. It suggests that partitioning of the appropriate C-space can be a powerful tool for analyzing the shortest path problem in more general and complex cases, as e.g. in finding the shortest path between a point and a manifold.

References

[1] M. Krein, A. Nudel'man, The Markov Moment Problem and Extremal Problems, The American Mathematical Society, Providence, RI, 1977.
[2] P. Jacobs, J. Canny, Planning smooth paths for mobile robots, in: Proceedings of the IEEE International Conference on Robotics and Automation, Scottsdale, AZ, May 1989.
[3] P. Jacobs, J. Laumond, M. Taix, Efficient motion planners for nonholonomic mobile robots, in: Proceedings of the IEEE/RSJ International Workshop on Intelligent Robots and Systems, Osaka, Japan, August 1991.
[4] J. Barraquand, J.-C. Latombe, On nonholonomic mobile robots and optimal maneuvering, in: Proceedings of the Fourth International Symposium on Intelligent Control, Albany, NY, 1989.
[5] L.E. Dubins, On curves of minimal length with a constraint on average curvature, and with prescribed initial and terminal positions and tangents, American Journal of Mathematics 79 (1957) 497–516.
[6] J.A. Reeds, L.A. Shepp, Optimal paths for a car that goes both forwards and backwards, Pacific Journal of Mathematics 145 (1990) 367–393.
[7] J. Boissonnat, A. Cerezo, J. Leblond, Shortest paths of bounded curvature in the plane, in: Proceedings of the IEEE International Conference on Robotics and Automation, Nice, France, May 1992.
[8] L.S. Pontryagin, The Mathematical Theory of Optimal Processes, Interscience, New York, 1962.
[9] G. Desaulniers, F. Soumis, An efficient algorithm to find a shortest path for a car-like robot, IEEE Transactions on Robotics and Automation 11 (6) (1995) 819–828.
[10] Ph. Soueres, J.-P. Laumond, Shortest paths synthesis for a car-like robot, IEEE Transactions on Automatic Control 41 (5) (1996) 672–688.

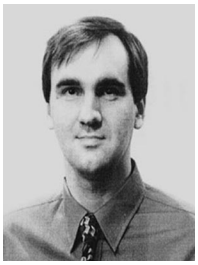

Andrei M. Shkel is an Assistant Professor in the Department of Mechanical and Aerospace Engineering and an Assistant Professor in the Department of Electrical and Computer Engineering at the University of California, Irvine. He is also the Director of the UCI Microsystems Laboratory. Dr. Shkel received his BS degree (magna cum laude) in Applied Mathematics in 1990 and MS degree in Applied Mechanics and Control in 1991, both from Lomonosov's Moscow State University. In 1997, he received PhD degree from the University of Wisconsin-Madison with major in Mechanical Engineering and allied in Electrical and Computer Engineering. The subject of his PhD was the sensor-based motion planning with kinematic and dynamic constraints. After receiving his PhD, Dr. Shkel joined Berkeley Sensor and Actuator Center (BSAC) as a Postdoctoral Researcher, where he was developing micro-machined monolithic gyroscopes. In 1999, Dr. Shkel joined the MEMSolutions, Inc., as a Senior MEMS Design Engineer, where he was conducting development and design of novel cost-effective sensors and optical MEMS-based products. He is currently a technical consultant for the MEMSolutions, Inc. Dr. Shkel is active in robotics, sensor-based intelligence, MEMS, and MEMS-based sensor technology. He served as a reviewer for more than a dozen major journals and international conferences in these areas, published 23 papers in archival journals and international conferences, and presented his work on a number of technical meetings and industry advisory boards. During the last 2 years, Dr. Shkel authored and co-authored five inventions (currently patents pending) on design of novel MEMS inertial sensors and optical MEMS-based products. Dr. Shkel is a member of the Administrative Committee of the IEEE Sensors Council, he is also an associate member of the IEEE and ASME.

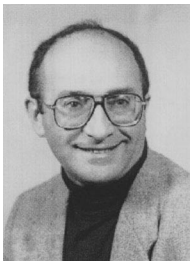

Vladimir J. Lumelsky is on the faculty at the University of Wisconsin-Madison, where he is Professor of Mechanical Engineering, Professor of Electrical Engineering, Professor of Computer Science, and Professor of Mathematics. He received his BS/MS in Electrical Engineering and Computer Science from the Institute of Precision Technology, Leningrad, Russia, and his PhD in Applied Mathematics from the Institute of Control Sciences (ICS), USSR National Academy of Sciences, Moscow, in 1970. He then held academic and research positions with the ICS, Moscow, Ford Motor Research Laboratories, General Electric Research Center, and Yale University. His professional interests, reflected in over 200 publications, include robotics, computational geometry, sensor-based intelligence, control theory, kinematics, industrial automation, computer vision, and pattern recognition. He has served on a number of editorial boards, including the Editor-in-Chief of *IEEE Sensors Journal* and Senior Editor of the *IEEE Transactions on Robotics and Automation*, on the Board of Governors of the IEEE Robotics and Automation Society, as Chairman of this Society's Technical Committee on Robot Motion Planning, Chairman of IFAC Working Group on Robot Motion, Sensing, and Planning, Program Chair of the 1989 IEEE International Conference on Intelligent Robots and Systems (IROS'89), Tokyo, Guest Editor for two special issues of the *IEEE Transactions on Robotics and Automation*. He is IEEE Fellow, and member of ACM and SME.